Dalton Transactions

ROYAL SOCIETY OF CHEMISTRY

PAPER

View Article Online
View Journal | View Issue

Cite this: *Dalton Trans.*, 2024, **53**, 4719

Lithium, sodium and potassium enolate aggregates and monomers: syntheses and structures†‡

Nathan Davison, Jack M. Hemingway, * Paul G. Waddell and Erli Lu *

Received 23rd January 2024,
Accepted 9th February 2024

DOI: 10.1039/d4dt00211c

rsc.li/dalton

In this *Article*, we report the syntheses and comparative structural studies of lithium, sodium, and potassium anthracen-9-yl enolates, as their aggregates (Li, Na: hexamer; K: tetramer) and ligand-stabilized monomers (for Li and Na). The monomers add new members to the rare collection of group-1 metal monomeric enolates. Moreover, the series covers different group-1 metal cations (Li^+, Na^+ and K^+) and aggregate sizes, allowing comparative structural studies to elucidate how the metal identity and aggregate size influence the enolate structure.

Introduction

Enolates derive from α-deprotonation of organocarbonyls, such as ketones and aldehydes. They are widespread reaction intermediates in organic chemistry, and enable several textbook organic reactions, such as aldol addition.[1] The most commonly used approach to generate enolates is the deprotonation of organocarbonyls using organo-alkali metal reagents, such as organolithium. The resultant alkali metal enolates are subsequently subjected to further transformations. It is quite understandable that the alkali metal enolate structures play an underpinning role in their following reactions. But the structural studies of isolated alkali metal enolates are not as well-established as one may expect: the state-of-the-art is covered in the following paragraph. Given the diverse scope of organocarbonyls (*e.g.*, ketones, aldehydes, esters, amides and so on), their derivative enolates feature a high level of structural diversity. Beyond the hydrocarbon enolates derived from ketones and aldehydes, heteroatom-substituted enolates, such as the ones derived from esters,[2] amides[3] or α-hetero organocarbonyls (*e.g.*, α-phosphino esters[4]), were also reported.

A key factor to influence the coordination complex structure is metal identity. For the enolate complexes, among the most common alkali metal cations Li^+, Na^+ and K^+, lithium enolates are the most studied. Since the 1980s, the groups of Williard,[5] Mulvey,[6] Reich,[7] Collum,[8] and Hevia,[9] among others,[10] reported a number of isolated and structurally characterized lithium enolate complexes, most of which are aggregates. In comparison with the relatively well-documented lithium enolates, sodium[5e,11] and potassium[5e,12] enolates are far less studied. A comparative structural study of Li, Na and K enolates within the same system, *i.e.*, the same enolate substitutions and the ligand, would help to unravel the metal identity's structural directing role. In 1986, Williard and Carpenter reported such a remarkable comparative study on a series of Li, Na and K enolates of pinacolone (*tert*-butyl methyl ketone).[13] In these cases, the Li and K pinacolone enolates were found to be hexamers (Li: no solvent coordination; K: one coordinated THF per K), while the Na enolate is a tetramer (no solvent coordination). The aggregates remain in solution as proven by NMR studies.[13] Despite clearly revealing "subtle structural differences" (according to the authors) induced by the metal identity, the work from Williard and Carpenter did not include another crucial comparison dimension: aggregate size.

Aggregate size is one of the most important structural factors in alkali metal chemistry, playing underpinning roles in the structure–reactivity relationship.[14] In the enolate chemistry specifically, as early as in 1981, Seebach and co-workers examined the mechanistic implications of the tetrameric cubic structure of Li enolates in addition reactions.[15,16] In 2013, Cossío and co-workers conducted computational studies (DFT and molecular dynamics) on the relationship between alkali metal enolates aggregate sizes and their activity (reaction rate) in the aldol addition,[17] where the monomers were found to be vastly superior to the dimers and tetramers. Out of the *in silico* chemical space, reported examples of crystallographically characterized alkali metal enolate monomers are rather

Chemistry-School of Natural and Environmental Sciences, Newcastle University, Newcastle upon Tyne, NE1 7RU, UK. E-mail: erli.lu@newcastle.ac.uk, jack.hemingway@newcastle.ac.uk; https://www.erlilulab.org

†This article is dedicated to Professor Chang-Tao Qian, Shanghai Institute of Organic Chemistry, on the occasion of his 90th birthday.

‡Electronic supplementary information (ESI) available. CCDC CCDC 2307285 (**3**-Li), 2307287 (**3**-Na), 2307288 (**3**-K), 2307289 (**6**-Li) and 2307290 (**6**-Na). For ESI and crystallographic data in CIF or other electronic format see DOI: https://doi.org/10.1039/d4dt00211c

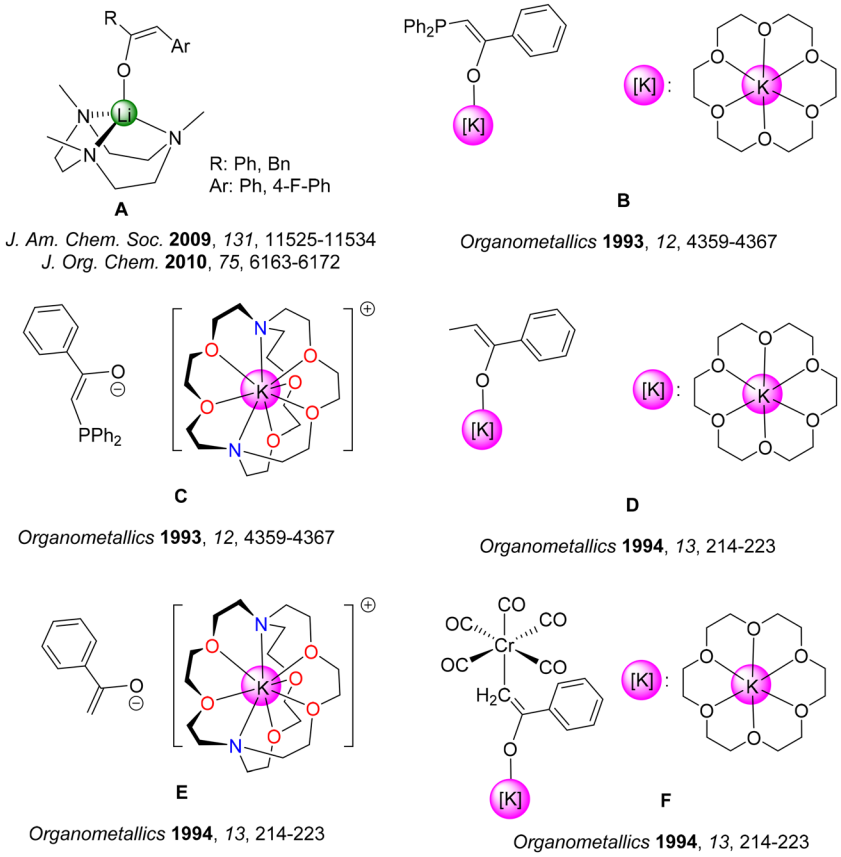

Fig. 1 The reported examples of Li and K enolate monomers.

limited. In 2009 and 2010, Reich and co-workers systematically studied the SCXRD and solution-state structures and the structural dynamics of several lithium enolates, with the presence of a series of ligands, including PMDTA, Me_3TACN (also known as TMTAN), HMPA, and cryptand [2.1.1].[7] The tridentate cyclic Me_3TACN ligand was found to be able to stabilize a collection of lithium enolate monomers[7] (Fig. 1A). Moving onto the heavier alkali metals, there is no sodium enolate monomer in literature, albeit a relevant sodium ethylacetoacetate monomer was reported as stabilized by 15-crown-5.[18] A few monomers of potassium enolates and α-heteroatom substituted enolates were reported in 1993 [4] and 1994 [12b,19] (Fig. 1B–F), including two separated ion pairs (Fig. 1C & E). Due to the scarcity of the alkali metal enolate monomers, an in-depth understanding of the structural differences between their aggregates and monomers remains an open question.

Since the 2020s, our group has focused on unravelling the structural and reactivity directing roles of the two key factors in alkali metal chemistry: (1) aggregate size;[20,21] (2) metal identity.[22] Herein, we bring the effort into Li, Na and K enolate chemistry by reporting the synthesis and characterisation of a series of Li, Na, K anthracen-9-yl enolates as their aggregates and ligand-stabilised monomers. We found that without external ligand, the Li and Na anthracen-9-yl enolates exist as hexamers but with different coordination geometries, while the K enolate exists as a tetramer. Employing the Me_6Tren ligand, we isolated and characterized two rare examples of Li and Na enolate monomers. Based on the complexes, the enolates structural trends are studied on two dimensions of comparison: (1) metal identity; (2) aggregate size. Our findings are elaborated in the following sections.

Results and discussion

Synthesis of the Li, Na and K enolates

As a part of our systematic studies of the Brønsted basicity and nucleophilicity of organo-alkali metal reagents,[20–22] 9-acetylanthracene (**1**) was treated with lithium, sodium and potassium alkyl complexes $[MCH_2SiMe_3]_n$ (M = Li, **2**-Li;[23] M = Na, **2**-Na;[24] M = K, **2**-K[25]) in d_6-benzene (for the NMR-scale reactions) or benzene (for the scale-up reactions) (Scheme 1). 9-Acetylanthracene was chosen as the substrate for its superior steric protection over the products, as well as the crystallinity induced by the anthracen-9-yl functional group. All the reactions occurred as deprotonation at the methyl position exclusively – we did not observe the possible nucleophilic addition side reaction towards the C=O bond. The corresponding Li,

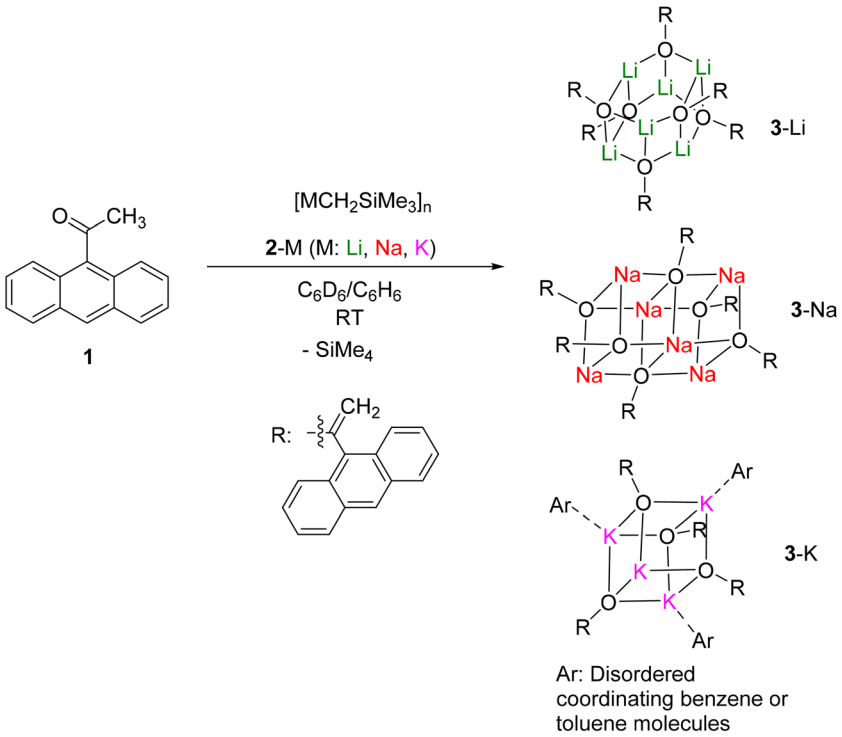

Scheme 1 Syntheses of Li, Na and K enolate clusters, **3**-Li (hexamer), **3**-Na (hexamer) and **3**-K (tetramer).

Na and K enolates, $[M\{OC(=CH_2)(C_{14}H_9)\}]_n$ (**3**-Li/Na/K, n = 6 for Li and Na, n = 4 for K), were isolated in 73–97% crystalline yields. Among them, **3**-Li and **3**-Na crystallize into hexamers, while **3**-K crystallizes as a tetramer. The ^{1}H and ^{7}Li (for **3**-Li) NMR spectra of **3**-Li/Na/K are reported in the ESI,‡ from the *in situ* ^{1}H NMR monitoring of the corresponding NMR-scale reaction. Upon formation, **3**-Li/Na/K crystallise from the C_6D_6/C_6H_6 solutions rapidly, and can not be re-dissolved. For this reason, their ^{13}C and ^{1}H DOSY NMR spectra are absent.

Following the successful syntheses of the enolate clusters **3**-Li/Na/K, reactions between **1** and the monomeric organo-alkali metal complexes, $[M(CH_2SiMe_3)(Me_6Tren)]$ (M = Li, **4**-Li;[26] M = Na, **4**-Na[22,27]) and $[K(CH_2Ph)(Me_6Tren)]$ (**5**-K[28]), were tested (Scheme 2). The **4**-Li/Na reactions yielded corresponding Me_6Tren-coordinated Li/Na enolate monomers, **6**-Li and **6**-Na, respectively. In comparison, reaction between a benzyl potassium monomer **5**-K[28] and **1** produced the potassium enolate tetramer **3**-K, while the Me_6Tren ligand dissociated and was observed in the ^{1}H NMR spectroscopy as coordination-free. We attribute the Me_6Tren ligand dissociation in the potassium reaction to two factors: (1) the relatively low affinity between the Me_6Tren ligand and K^+ (comparing with Li^+/Na^+): the low affinity between Me_6Tren and K^+ allowed us to realize the first alkali metal cations selective reduction between K^+ and Li^+;[29] (2) The K enolate tetramer **3**-K structure features much more significant cation–arene interactions (*vide infra*, Fig. 4) comparing with the structures of **3**-Li (Fig. 2) and **3**-Na (Fig. 3). The alkali metal cation–arene interaction is known to be more pronounced for heavier alkali metal cations.[21b,28,30]

Single-crystal X-ray diffraction (SCXRD) structures of the Li, Na and K enolates

The hexameric (**3**-Li, **3**-Na), tetrameric (**3**-K) and monomeric (**6**-Li, **6**-Na) structures were confirmed by the SCXRD studies: their solid-state molecular structures are presented in Fig. 2–6. In the following section, we will focus on the structural influences induced by two factors: (i) the metal identity; (ii) the aggregate size. In the aggregate clusters **3**-Li/Na/K, we did not observe pronounced π–π stacking[31] between the anthracenyl substitutes, or with the coordinated arene solvents. Hence, the π–π stacking is not a major structural contributor and therefore, we are confident that the trends summarized in the following section are not only limited to the anthracen-9-yl enolate, but also extrapolatable to other enolates.

The influence of the metal's identity is obvious for enolate clusters **3**-Li/Na/K, especially in their aggregate sizes and geometries. For the smallest Li^+, the enolate hexamer **3**-Li features a Li_6O_6 hexagonal prismatic core (Fig. 2), which is similar to a Li pinacolone enolate hexamer reported by Williard and coworkers.[5h] In **3**-Li, each Li center coordinates with three O sites and features a coordination number of three. Upon moving from Li^+ to Na^+, one may expect the metal's coordination number to increase with the increase of metal's ionic radius. Indeed, **3**-Na features a three-deck square prismatic structure (Fig. 3), with the inner deck Na^+ centers featuring a coordination number of four, while the outer decks Na^+ centers' coordination number is three. While **3**-Li and **3**-Na can also be considered as two stacked layers of M_3O_3 motif, it

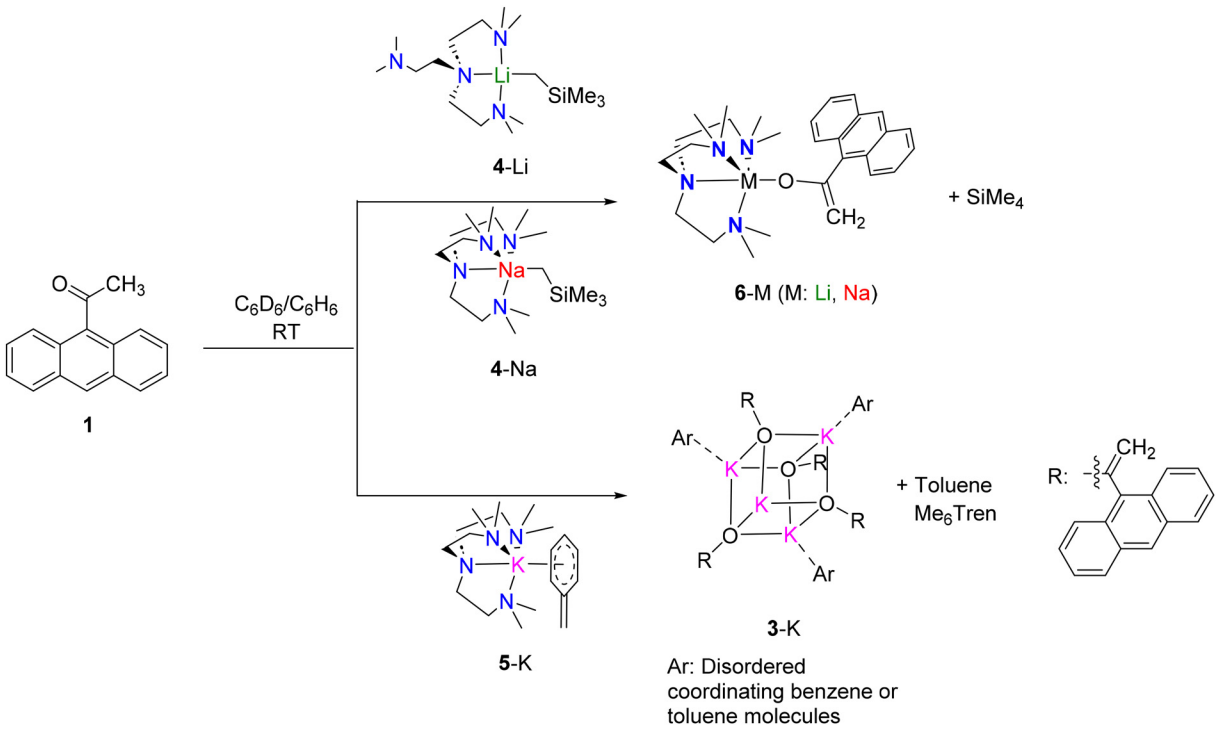

Scheme 2 Syntheses of Li and Na enolate monomers **6**-Li/Na.

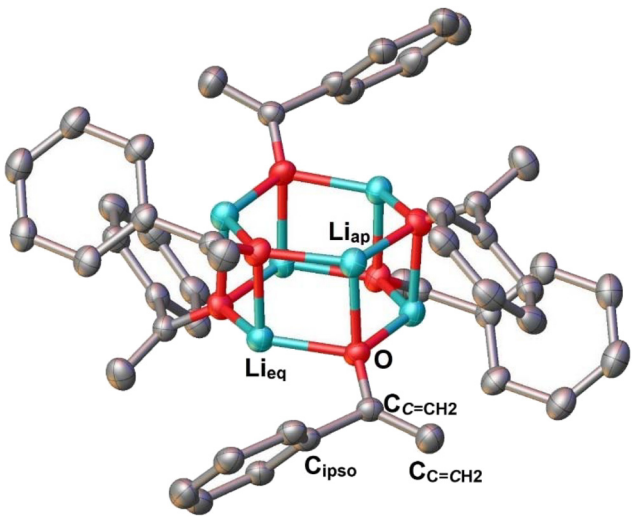

Fig. 2 The SCXRD structure of **3**-Li. Hydrogen atoms, solvent benzene molecules in the lattice, and the two flanking phenyl rings of the anthracene are omitted for clarity. Only one third of the molecule is labelled, but the whole molecule is crystallographically independent. To facilitate readers, we labelled the atoms in a chemically intuitive way, instead of using the numeric atomic number system. The atomic numbers can be found in the Cambridge Structural Database archive. Key bond lengths are provided as ranges: Li_{ap}–O (1.95–1.97 Å), Li_{eq}–O (1.85–1.92 Å), O–$C_{C=CH_2}$ (1.34–1.35 Å), $C_{C=CH_2}$–$C_{C=CH_2}$ (1.31–1.33 Å), $C_{C=CH_2}$–C_{ipso} (1.49–1.51 Å).

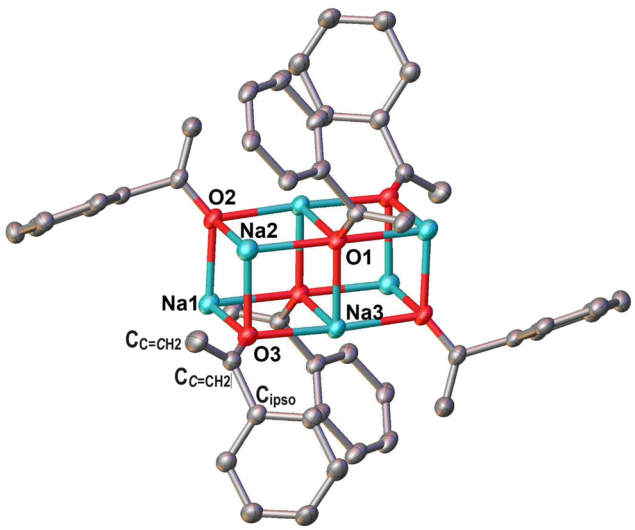

Fig. 3 The SCXRD structure of **3**-Na. Hydrogen atoms, solvent benzene molecules in the lattice, and the two flanking phenyl rings of the anthracene are omitted for clarity. Half of the whole molecule is crystallographically independent, while the key independent atoms are labelled. Key bond lengths are provided as ranges: Na–O (2.24–2.38 Å), O–$C_{C=CH_2}$ (1.32–1.33 Å), $C_{C=CH_2}$–$C_{C=CH_2}$ (1.33–1.34 Å), $C_{C=CH_2}$–C_{ipso} (1.49–1.51 Å).

is interesting to compare the M_3O_3 layer structures (Scheme 3). The larger Na^+ cation leads to longer Na–O bond, which "tethers" the M and O in the middle of the M_3O_3 unit (Scheme 3). From another perspective, **3**-Li is a "ring-laddering" loop, while **3**-Na features a "ring-stacking" structure (Scheme 3). It worth mentioning that the ring-laddering and ring-stacking are ubiquitous structural features in group-1 metal coordination chemistry and have been well documen-

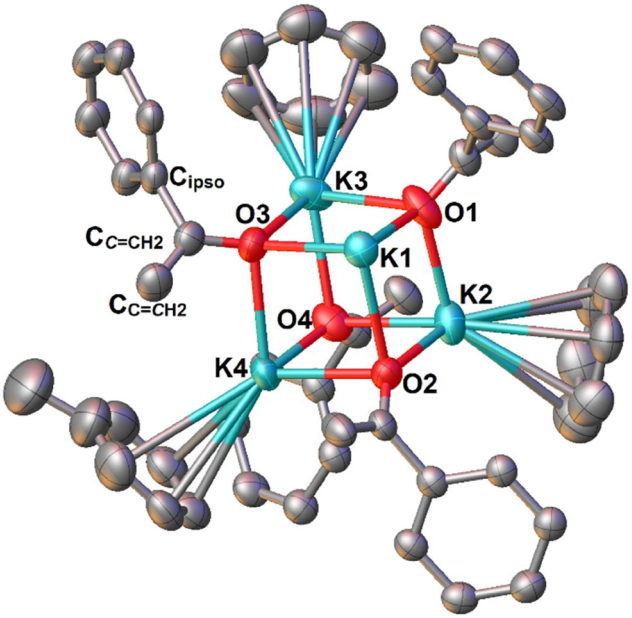

Fig. 4 The SCXRD structure of **3**-K. Hydrogen atoms, solvent benzene molecules in the lattice, and the two flanking phenyl rings of the anthracene are omitted for clarity. Both benzene and toluene molecules occupying the same positions throughout the crystal manifesting as disorder. The asymmetric unit also contains a solvent-accessible void in which there appear to be multiple orientations of both toluene and benzene. An unambiguous model for these solvent molecules in this site could not be achieved and hence the associated electron density was treated using the Olex2 solvent mask routine. To facilitate readers, we labelled the atoms in a chemically intuitive way, instead of using numeric numbers. Key bond lengths are provided as ranges: K–O (2.51–2.75 Å), O–$C_{C=CH_2}$ (1.29–1.31 Å), $C_{C=CH_2}$–$C_{C=CH_2}$ (1.33–1.34 Å), $C_{C=CH_2}$–C_{ipso} (1.50–1.52 Å).

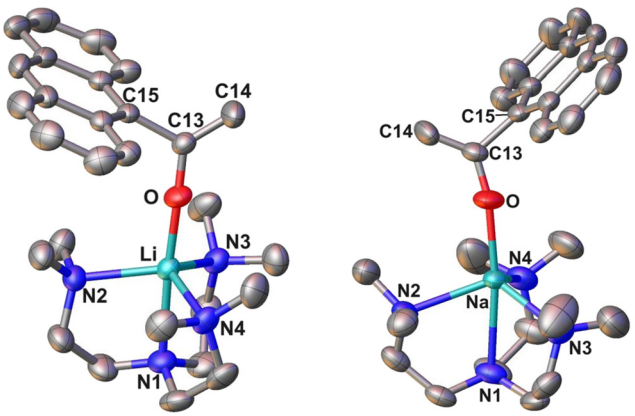

Fig. 5 The SCXRD structure of **6**-Li (left) and **6**-Na (right). Hydrogen atoms and solvent molecules in the lattice are omitted for clarity. Key bond lengths: **6**-Li: Li–O (1.827(2) Å), O–C13 (1.2836(13) Å), C13–C14 (1.3389(18) Å), C13–C15 (1.5148(14) Å); **6**-Na: Na–O (2.1324(18) Å), O–C13 (1.279(3) Å), C13–C14 (1.343(3) Å), C13–C15 (1.521(3) Å).

ted.[32] Reviewing the literature[33] suggests that the determining factor is metal identity, or more specifically, the metal ionic radius, as we observed herein; though influences from ligand atom (*e.g.*, C *vs.* N *vs.* O) and ligand steric profile should also be considered.

A further increase in the ionic radius going from Na^+ to K^+ leads into a distorted cubic K_4O_4 core in 3-K (Fig. 4), which features significant cation–π interactions with the arene solvent molecules. It is interesting to note that both benzene and toluene solvent molecules coordinate to the K centers (albeit disordered), and only three out of the four K centers are coordinated by the arene solvent molecules. This solvent molecule coordination discrimination, *i.e.*, not all the K centres are coordinated, results in an asymmetric K_4O_4 core, and could likely be a result of steric crowding. The cation–π interaction is much more pronounced in **3**-K than in **3**-Li/Na (not at all for **3**-Li, very little Na-anthracenyl interactions in **3**-Na), which can be attributed to the stronger π-affinity of K^+.[21b,28] Compared with the pronounced metal identity structural influence in the aggregate size and geometry, the anionic enolate ligand structure, $[OC(=CH_2)(C_{14}H_9)]^-$, in **3**-Li/Na/K, is largely unaffected by changes of the metal identity and the resultant changes of aggregate size. But we did observe non-negligible differences of the anionic enolate ligand structure between the clusters **3**-Li/Na and the monomers **6**-Li/Na, which will be elaborated in the following paragraphs.

The enolate monomers **6**-Li/Na share a similar five-coordinate core structure (Fig. 5), where the Me_6Tren ligand's four nitrogen atoms and the oxygen atom of the enolate ligand furnish the inner coordination sphere. The Na–N/O bonds in **6**-Na are longer than the corresponding Li–N/O bonds in **6**-Li, reflecting sodium's larger ionic radius. The geometries of enolate ligand in **6**-Li/Na are very similar, which is also reflected by the density functional theory (DFT) charge distribution studies. Examining the natural bonding orbital (NBO) atomic charges for the modelled monomers **6′**-Li/Na indicates little differences between the Li and Na complexes (Fig. 6). For both **6′**-Li and **6′**-Na, a positive charge of approximately 0.9 is located on the metal cation, and a countering negative charge is located on the oxygen atom.

However, despite being largely immune to the change of metal identity, the enolate ligand structure can be influenced by the aggregate size. By comparing the enolate units in the hexamers (**3**-Li/Na) and monomers (**6**-Li/Na), we noted that the C–O bonds are significantly shorter in the monomers (monomers 1.27–1.28 Å *vs.* hexamers 1.32–1.35 Å) (Scheme 4). While the C=C and C–Ar bonds appear as slightly longer in the monomers, these elongation (0.01–0.02 Å) are too small to be considered as pronounced. The shortening of C–O bond in the monomers could be attributed to a weaker stabilization of the negative charge on the oxygen *cf.* the hexamers: In the hexamers, each anionic oxygen is coordinated by three (**3**-Li) or four (**3**-Na) metal cations, but the number is one in the monomers.

To further understand whether there is a thermodynamic preference between the liner and the bent M–O–C angles, or if it is largely kinetic-driven (*i.e.*, depends on the steric congestion), we conducted potential energy surface scans. The meth-

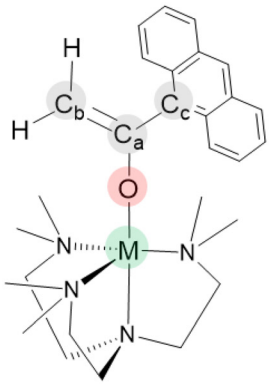

	M	O	C_a	C_b	C_c
M = Li	0.879	-0.933	0.348	-0.688	0.005
M = Na	0.906	-0.918	0.336	-0.691	0.010

Fig. 6 NBO charge per atom from natural population analyses of **6′**-Li and **6′**-Na.

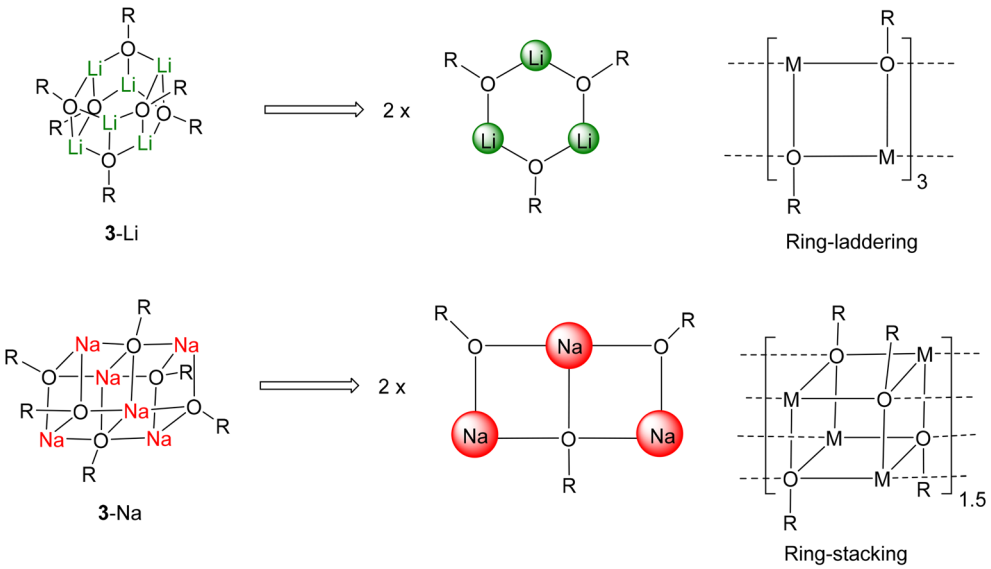

Scheme 3 The M_3O_3 unit in **3**-Li and **3**-Na, and the ring-laddering (**3**-Li) and ring-stacking (**3**-Na) representation of the complexes.

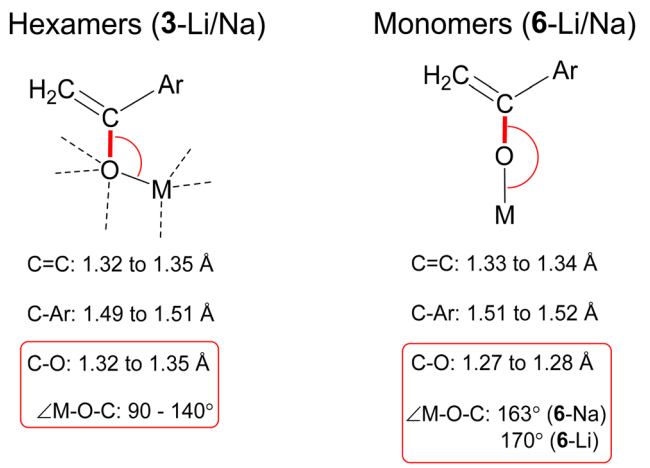

Scheme 4 Comparing the bond lengths in the enolate units of the hexamers and the monomers. The most pronounced structural changes are observed in the C–O bond length and the M–O–C bond angle (highlighted in red).

odology has been well-established to probe the energetic preference for *cis* or *trans* conformations in coordination chemistry.[34] The calculations are based on the hypothetical model of the monomeric M–O–C(=CH_2)Ar (Ar: anthracenyl), which removes all the ligand and secondary bridging units, minimizing the steric influence. The M–O–C angle was initially set to 90° leaving the remainder of the M–O–C(=CH_2)Ar moiety unchanged from the optimized structure and was then sequentially increased by 5° until equal to 270°. All geometric parameters were relaxed to loose convergence criteria at each angle step except the M–O–C angle itself which was fixed. It was found that the minimum energy of M–O–C(=CH_2)Ar was at 205° regardless of the metal identity, with the near linear structures being favored over the more bent structures. The resulting plots are shown in Fig. 7. We also observed that the 90° angle (metal cation pointing towards the C=CH_2 unit) is preferred over the 270° angle (metal cation pointing towards the aryl), which could be a result of steric repulsion between the bulky anthracenyl and the metal cation.

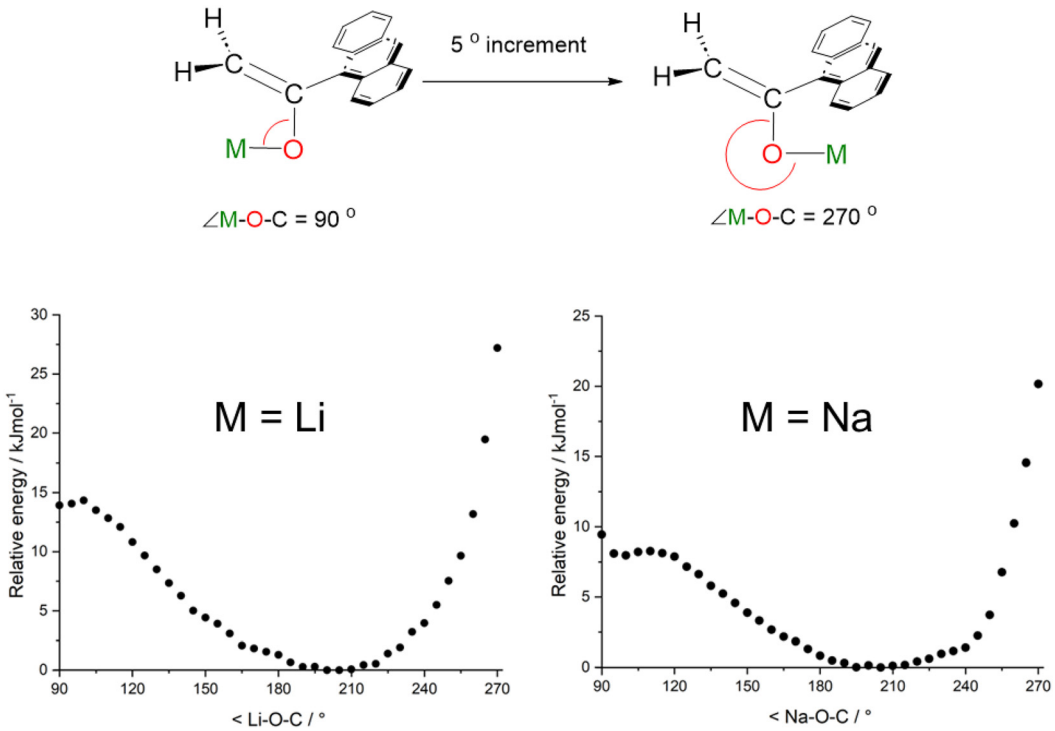

Fig. 7 Potential energy surface scans of the M–O–C angle M–O–C(=CH_2)Ar (M = Li – left and M = Na – right).

Conclusion

Herein, we report the syntheses and structures of a series of Li, Na and K enolates. Without any external ligand, the enolates aggregate into hexamers (Li and Na) and tetramer (K), and their geometries are heavily influenced by the metal identity, as well as the particularly pronounced metal cation–arene interactions in the potassium case. With the presence of the Me_6Tren ligand, the Li and Na enolates exist as monomers with similar structures. The coordination of the Me_6Tren ligand to Li^+ or Na^+ is the key to form the monomeric structures. In comparison, the Me_6Tren ligand failed to coordinate to K^+, hence the corresponding K enolate monomer is not available.

This work adds five new members to the alkali metal enolate family. In particular, the two monomers **6**-Li and **6**-Na are the newest examples of the scarce collection of alkali metal enolate monomers. The aggregates, **3**-Li/Na/K, exhibit a clear structural trend dictated by the metal identity, specifically, the metal ionic radius. Comparisons between the monomers **6**-Li/Na and their corresponding hexamers **3**-Li/Na unveils an interesting influence of the aggregate size towards the carbon–oxygen bond length in the enolate ligand. It would be interesting to see how the structural observations in this work would be translated into the enolate reactivity – more investigations are underway and will be reported in due course.

Author contributions

E. L. and N. D. conceived and conceptualised the studies. N. D. conducted the syntheses and experimental characterisations under E. L.'s supervision. J. M. H. designed and conducted the computational studies under the guidance of E. L. P. G. W. collected and refined and the single-crystal X-ray diffraction data. E. L. wrote the manuscript with input from all the authors.

Conflicts of interest

There are no conflicts to declare.

Acknowledgements

The authors thank the Chemistry Technical Support Team (Drs Laura McCorkindale and Amy Roberts, Mr Niall Straughan) at Newcastle University for supporting our research. E. L., N. D. and J. M. H. thank the Newcastle University Academic Track (NUAcT) Fellowship (E. L. and N. D.) and the Leverhulme Trust (RPG-2022-231) for financial support.

References

1 For example, a lithium "aldolate", *i.e.*, the aldol addition intermediate, was isolated and characterized in 1985: P. G. Williard and J. M. Salvino, X-Ray Crystal Structure of a Lithium Aldolate – A Tetrameric Aggregate, *Tetrahedron Lett.*, 1985, **26**, 3931–3934.

2 D. Seebach, R. Amstutz, T. Laube, B. Schweizer and J. D. Dunitz, Structures of Three Lithium Ester Enolates by X-ray Diffraction: Derivation of Reaction Path for Cleavage into Ketene and Alcoholate, *J. Am. Chem. Soc.*, 1985, **107**, 5403–5409.

3 W. Bauer, T. Laube and D. Seebach, Crystal and molecular structure of a THF-solvated lithium amide enolate dimer, *Chem. Ber.*, 1985, 764–773.

4 P. Veya, C. Floriani, A. Chiesi-Villa, C. Guastini, A. Dedieu, F. Ingold and P. Braunstein, Experimental and Theoretical Studies on the Reactivity of α-Phosphino Enolates. Crystal Structures of [K(18-crown-6)][Ph_2PCHC(O)Ph] and [K(Kryptofix-2,2,2)][Ph_2PCHC(O)Ph], *Organometallics*, 1993, **12**, 4359–4367.

5 (*a*) P. G. Williard and G. B. Carpenter, X-ray Crystal Structure of an Unsolvated Lithium Enolate Anion, *J. Am. Chem. Soc.*, 1985, **107**, 3345–3346; (*b*) P. G. Williard and M. J. Hintze, The First Structural Characterization of a Dimeric Lithium Ketone Enolate-Lithium Diisopropylamide Complex, *J. Am. Chem. Soc.*, 1987, **109**, 5539–5541; (*c*) P. G. Williard and G. J. MacEwan, Crystal Structure of a Unique Aggregate Containing Lithium and Potassium Cations, Ketone Enolate, and *tert*-Butoxide, *J. Am. Chem. Soc.*, 1989, **111**, 7671–7672; (*d*) P. G. Williard and M. J. Hintze, Mixed Aggregates: Crystal Structures of a Lithium Ketone Enolate/Lithium Amide and of a Sodium Ester Enolate/Sodium Amide, *J. Am. Chem. Soc.*, 1990, **112**, 8602–8604; (*e*) K. W. Henderson, P. G. Williard and P. R. Bernstein, Synthesis and Characterization of the First Mixed Alkali Metal Enolate Containing Amine Ligands: A Novel "Open-Stack" Structure and Its Implications for Aldol Addition, *Angew. Chem., Int. Ed. Engl.*, 1995, **34**, 1117–1119; (*f*) K. W. Henderson, A. E. Dorigo, P. G. Williard and P. R. Bernstein, A Triple Anion Complex Containing Enolate, Amide, and Halide – A New Structural Type in Lithium Chemistry, *Angew. Chem., Int. Ed. Engl.*, 1996, **35**, 1322–1324; (*g*) J. Guang, Q. P. Liu, R. Hopson and P. G. Williard, Lithium Pinacolone Enolate Solvated by Hexamethylphosphoramide, *J. Am. Chem. Soc.*, 2015, **137**, 7347–7356; (*h*) J. Guang, Q. Liu, R. Hopson, G. Kagan, W. Li, T. B. Monroe and P. G. Williard, Conformational Polymorphism of Lithium Pinacolone Enolate, *J. Am. Chem. Soc.*, 2016, **138**, 15177–15188.

6 W. Clegg, L. Horsburgh, R. E. Mulvey and M. J. Ross, Crystal Structure of Dilithioacetylacetone: A Twenty-Four Vertex Li-O Cage Molecule with Limited Li-C(terminal) Bonding and Selective THF Solvation, *Angew. Chem., Int. Ed. Engl.*, 1995, **34**, 1233–1234.

7 (*a*) K. J. Kolonko, M. M. Biddle, I. A. Guzei and H. J. Reich, Solution Structures of Lithium Enolates of Cyclopentanone, Cyclohexanones, Acetophenones, and Benzyl Ketones. Triple Ions and Higher Lithiate Complexes, *J. Am. Chem. Soc.*, 2009, **131**, 11525–11534; (*b*) K. J. Kolonko, I. A. Guzei and H. J. Reich, Structure and Dynamics of α-Aryl Amide and Ketone Enolates: THF, PMDTA, TMTAN, HMPA, and Crypt-Solvated Lithium Enolates, and Comparison with Phosphazenium Analogues, *J. Org. Chem.*, 2010, **75**, 6163–6172.

8 N. M. Lui, S. N. MacMillan and D. B. Collum, Lithiated Oppolzer Enolates: Solution Structures, Mechanism of Alkylation, and Origin of Stereoselectivity, *J. Am. Chem. Soc.*, 2022, **144**, 23379–23395.

9 D. R. Armstrong, A. M. Drummond, L. Balloch, D. V. Graham, E. Hevia and A. R. Kennedy, Metalation of 2,4,6-Trimethylacetophenone Using Organozinc Reagents: The Role of the Base in Determining Composition and Structure of the Developing Enolate, *Organometallics*, 2008, **27**, 5860–5866.

10 (*a*) J. T. B. H. Jastrzebski, G. van Koten, M. J. N. Christophersen and C. H. Stam, The Unexpected Formation of a Lithium-Enolate from Bis{2-[(Dimethylamino)Methyl]Phenyl} Copper Lithium. X-ray Structure of $Li_4[OC(=CH_2)C_6H_4CH2NMe_2\text{-}2]_4$, *J. Organomet. Chem.*, 1985, **292**, 319–324; (*b*) P. J. Posposil, S. R. Wilson and E. N. Jacobsen, A Substoichiometric Pyridine-Lithium Enolate Complex: Solution and X-ray Data and Implications for Catalysis in Aldol Reaction, *J. Am. Chem. Soc.*, 1992, **114**, 7585–7587; (*c*) M.-L. Hsueh, B.-T. Ko, T. Athar, C.-C. Lin, T.-M. Wu and S.-F. Hsu, Synthesis, Structure, and Catalysis Studies of Mixed Lithium-Magnesium and Sodium-Magnesium Complexes: Highly Isospecific Initiators for Polymerization of Methyl Methacrylate, *Organometallics*, 2006, **25**, 4144–4149; (*d*) R. Knorr and M. Knittl, Unusual (3 THF)-microsolvated dimers and donor-free aggregates of two lithium enolates, *Tetrahedron*, 2021, **102**, 132500; (*e*) S. Zhou, X. Xu, X. Zhu, Y. Zheng, S. Chen and M. Xue, A facile approach to *C*-functionalized β-ketoimine compounds *via* terminal alkylation of a tetralithiated intermediate, *Org. Biomol. Chem.*, 2022, **20**, 4289–4292.

11 (*a*) E. Hevia, K. W. Henderson, A. R. Kennedy and R. E. Mulvey, Synthesis and Characterization of New Mixed-Metal Sodium-Magnesium Enolates Derived from 2,4,6-Trimethylacetophenone, *Organometallics*, 2006, **25**, 1778–1785; (*b*) S. E. Baillie, E. Hevia, A. R. Kennedy and R. E. Mulvey, Synthesis of Mixed Alkali-Metal-Zinc Enolate Complexes Derived from 2,4,6-Trimethylacetophenone: New Inverse Crown Structures, *Organometallics*, 2007, **26**, 204–209; (*c*) S. K. Ray, A. Homberg, M. Vishe, C. Besnard and J. Lacour, Efficient Synthesis of Ditopic Polyamide Receptors for Cooperative Ion Pair Recognition in Solution and Solid States, *Chem. – Eur. J.*, 2018, **24**, 2944–2951; (*d*) A. Homberg, R. Hrdina, M. Vishe, L. Guénée and J. Lacour, Stereoselective deconjugation of macrocyclic α,β-unsaturated esters by sequential amidation and olefin

transposition: application to enantioselective phase-transfer catalysis, *Org. Biomol. Chem.*, 2019, **17**, 6905–6910; (*e*) R. A. Woltornist and D. B. Collum, Ketone Enolization with Sodium Hexamethyldisilazide: Solvent- and Substrate-Dependent E–Z Selectivity and Affiliated Mechanisms, *J. Am. Chem. Soc.*, 2021, **143**, 17452–17464.

12 (*a*) E. Hevia, K. W. Henderson, A. R. Kennedy and R. E. Mulvey, Synthesis and Characterization of New Mixed-Metal Sodium-Magnesium Enolates Derived from 2,4,6-Trimethylacetophenone, *Organometallics*, 2006, **25**, 1778–1785; (*b*) S. E. Baillie, E. Hevia, A. R. Kennedy and R. E. Mulvey, Synthesis of Mixed Alkali-Metal-Zinc Enolate Complexes Derived from 2,4,6-Trimethylacetophenone: New Inverse Crown Structures, *Organometallics*, 2007, **26**, 204–209; (*c*) S. K. Ray, A. Homberg, M. Vishe, C. Besnard and J. Lacour, Efficient Synthesis of Ditopic Polyamide Receptors for Cooperative Ion Pair Recognition in Solution and Solid States, *Chem. – Eur. J.*, 2018, **24**, 2944–2951; (*d*) A. Homberg, R. Hrdina, M. Vishe, L. Guénée and J. Lacour, Stereoselective deconjugation of macrocyclic α,β-unsaturated esters by sequential amidation and olefin transposition: application to enantioselective phase-transfer catalysis, *Org. Biomol. Chem.*, 2019, **17**, 6905–6910; (*e*) R. A. Woltornist and D. B. Collum, Ketone Enolization with Sodium Hexamethyldisilazide: Solvent- and Substrate-Dependent E–Z Selectivity and Affiliated Mechanisms, *J. Am. Chem. Soc.*, 2021, **143**, 17452–17464.

13 P. J. Williard and G. B. Carpenter, X-ray Crystal Structures of Lithium, Sodium, and Potassium Enolates of Pinacolone, *J. Am. Chem. Soc.*, 1986, **108**, 462–468.

14 H. J. Reich, Role of Organolithium Aggregates and Mixed Aggregates in Organolithium Mechanisms, *Chem. Rev.*, 2013, **113**, 7130–7178.

15 D. Seebach, R. Amstutz and J. D. Dunitz, Tetrameric Cubic Structures of Two Solvated Lithium Enolates, *Helv. Chim. Acta*, 1981, **64**, 2617–2621.

16 R. Amstutz, W. B. Schweizer and D. Seebach, Mechanistic Implications of the Tetrameric Cubic Structure of Lithium Enolates, *Helv. Chim. Acta*, 1981, **64**, 2622–2626.

17 O. Larrañaga, A. de Cózer, F. M. Bickelhaupt, R. Zangi and F. P. Cossío, Aggregation and Cooperative Effects in the Aldol Reactions of Lithium Enolates, *Chem. – Eur. J.*, 2013, **19**, 13761–13773.

18 C. Cambillau and G. Bram, Complexes formés par addition d'éthers-couronnes aux énolates de Na^+ et K^+ de l'acétylacétate d'éthyle: structures cristallines et système d'équilibres en solution dans le THF et le DMSO, *Can. J. Chem.*, 1982, **60**, 2554–2565.

19 P. Veya and C. Floriani, Reaction of Metal Carbonyls with Naked Enolates to Make a Metallocarbene Enolate and ALkylcarbonylmetalates, *Organometallics*, 1994, **13**, 214–223.

20 For a review, see: N. Davison and E. Lu, The quest for organo-alkali metal monomers: unscrambling the structure-reactivity relationship, *Dalton Trans.*, 2023, **52**, 8172–8192.

21 For representative reports, see: (*a*) N. Davison, E. Falbo, P. G. Waddell, T. J. Penfold and E. Lu, A monomeric methyllithium complex: synthesis and structure, *Chem. Commun.*, 2021, **57**, 6205–6208; (*b*) J. Barker, N. Davison, P. G. Waddell and E. Lu, Monomeric lithium and sodium silylbenzyl complexes: synthesis, structures, and C=O bond olefination, *Chem. Commun.*, 2023, **59**, 8083–8086.

22 N. Davison, C. L. McMullin, L. Zhang, S.-X. Hu, P. G. Waddell, C. Wills, C. Dixon and E. Lu, Li vs Na: Distinct Reaction Patterns of Organo-Lithium and -Sodium Monomeric Complexes, and Ligand-Catalyzed Ketone/Aldehyde Methylenation, *J. Am. Chem. Soc.*, 2023, **145**, 6562–6576.

23 P. J. Davidson, D. H. Harris and M. F. Lappert, Subvalent Group 4B metal alkyls and amides. Part I. The synthesis and physical properties of kinetically stable bis[bis(trimethysilyl)methyl]-germanium(II), -tin(II), and -lead(II), *J. Chem. Soc., Dalton Trans.*, 1976, 2268–2274.

24 (*a*) S. E. Baillie, W. Clegg, P. García-Álvarez, E. Hevia, A. R. Kennedy, J. Klett and L. Russo, Synthesis and characterization of an infinite sheet of metal–alkyl bonds: unfolding the elusive structure of an unsolvated alkali-metal trisalkylmagnesiate, *Chem. Commun.*, 2011, **47**, 388–390; (*b*) J. R. Lynch, A. R. Kennedy, J. Barker, J. Reid and R. E. Mulvey, Crystallographic Characterisation of Organolithium and Organomagnesium Intermediates in Reactions of Aldehydes and Ketones, *Helv. Chim. Acta*, 2022, **105**, e202200082.

25 W. Clegg, B. Conway, A. R. Kennedy, J. Klett, R. E. Mulvey and L. Russo, Synthesis and Structures of [(Trimethylsilyl)methyl]sodium and -potassium with Bi- and Tridentate N-Donor Ligands, *Eur. J. Inorg. Chem.*, 2011, 721–726.

26 N. Davison, P. G. Waddell, C. Dixon, C. Wills, T. J. Penfold and E. Lu, A monomeric (trimethylsilyl)methyl lithium complex: synthesis, structure, decomposition and preliminary reactivity studies, *Dalton Trans.*, 2022, **51**, 10707–10713.

27 D. E. Anderson, A. Tortajada and E. Hevia, Highly Reactive Hydrocarbon Soluble Alkylsodium Reagents for Benzylic Aroylation of Toluenes using Weinreb Amides, *Angew. Chem., Int. Ed.*, 2023, **62**, e202218498.

28 M. G. Davidson, D. Garvia-Vivo, A. R. Kennedy, R. E. Mulvey and S. D. Robertson, Exploiting σ/π Coordination Isomerism to Prepare Homologous Organoalkali Metal (Li, Na, K) Monomers with Identical Ligand Sets, *Chem. – Eur. J.*, 2011, **17**, 3364–3369.

29 N. Davison, P. G. Waddell and E. Lu, Reduction of K^+ or Li^+ in a Heterobimetallic Electride $K^+[LiN(SiMe_3)_2]e^-$, *J. Am. Chem. Soc.*, 2023, **145**, 17007–17012.

30 D. E. Anderson, A. Tortajada and E. Hevia, New Frontiers in Organosodium Chemistry as Sustainable Alternatives to Organolithium Reagents, *Angew. Chem., Int. Ed.*, 2023, e202313556.

31 For a recent review on π–π and other stacking effects in coordination chemistry, especially their structure-directing roles, see: D. P. Malenov and S. D. Zarić, Stacking inter-

actions of aromatic ligands in transition metal complexes, *Coord. Chem. Rev.*, 2020, **419**, 213338.

32 For the ring-laddering and ring-stacking concept, see: (*a*) D. Barr, W. Clegg, R. E. Mulvey, R. Snaith and K. Wade, Bonding implications of interatomic distances and ligand orientations in the iminolithium hexamers $[LiN{=}C(Ph)^tBu]_6$ and $[LiN{=}C(Ph)NMe_2]_6$: a stacked-ring approach to these and related oligomeric organolithium systems, *J. Chem. Soc., Chem. Commun.*, 1986, 295–297; (*b*) R. E. Mulvey, Ring-Stacking and Ring-Laddering in Organonitrogenlithium Compounds: The Development of Concepts with Wide Applicability throughout Lithium Structural Chemistry, *Chem. Soc. Rev.*, 1991, **20**, 167–209; (*c*) R. E. Mulvey, Synthetic and structural developments in hetero-s-block-metal chemistry: new ring-laddering, ring-stacking and other architectures, *Chem. Soc. Rev.*, 1998, **27**, 339–346; (*d*) A. D. Bond, Ring-Laddering and Ring-Stacking: Unifying Concepts in the Structural Chemistry of Organic Ammonium Halides, *Cryst. Growth Des.*, 2005, **5**, 755–771.

33 (*a*) W. N. Setzer and P. v. R. Schleyer, X-Ray Structural Analyses of Organolithium Compounds, *Adv. Organomet. Chem.*, 1985, **24**, 353–451; (*b*) C. Schade and P. v. R. Schleyer, Sodium, Potassium, Rubidium, and Cesium: X-Ray Structurai Analysis of Their Organic Compounds, *Adv. Organomet. Chem.*, 1987, **27**, 169–278; (*c*) K. Gregory, P. v. R. Schleyer and R. Snaith, Structures of Organonitrogen—Lithium Compounds: Recent Patterns and Perspectives in Organolithium Chemistry, *Adv. Inorg. Chem.*, 1991, **37**, 47–142.

34 (*a*) E. Lu, O. J. Cooper, F. Tuna, A. J. Wooles, N. Kaltsoyannis and S. T. Liddle, Uranium-Carbene-Imido Metalla-Allenes: Ancillary-Ligand-Controlled cis-/trans-Isomerisation and Assessment of trans Influence in the $R_2C{=}U(IV){=}NR'$ Unit ($R{=}Ph_2PNSiMe_3$; $R'{=}CPh_3$), *Chem. – Eur. J.*, 2016, **22**, 11559–11563; (*b*) E. Lu, S. Sajjad, V. E. J. Berryman, A. J. Wooles, N. Kaltsoyannis and S. T. Liddle, Emergence of the structure-directing role of f-orbital overlap-driven covalency, *Nat. Commun.*, 2019, **10**, 634.